Peculiarities in the structure - properties relationship of epoxy-silica hybrids with highly organic siloxane domains

F. Piscitelli[1,2], G.G. Buonocore[1], M. Lavorgna[1]*, L.Verdolotti[1], S. Pricl[3], G. Gentile[1] and L. Mascia[4]

[1] *Institute of Polymers, Composites and Biomaterials, National Research Council, P.le E. Fermi, 1, 80155 Portici, Napoli, Italy*

[2] *Italian Aerospace Research Center (CIRA), Via Maiorise 81043 Capua (Caserta), Italy*

[3] *Molecular Simulations Engineering (MOSE) Laboratory – DEA, Piazzale Europa 1, 34127 Trieste, Italy*

[4]*Department of Materials, Loughborough University, Loughborough, LE11 3TU, United Kingdom*

Corresponding Author: Marino Lavorgna

mlavorgn@unina.it

Abstract

Epoxy-silica hybrids were produced from a diglycidyl ether of bisphenol-A resin using Jeffamine 230 hardener with a two-step *in situ* generation of siloxane domains. The siloxane component was obtained by hydrolysis and condensation of a mixture of γ-glycidoxypropyl-trimethoxysilane and tetraethoxysilane, which was added to the epoxy resin after removal of the formed alcohols and water. The morphological structure of the hybrids was examined by TEM, SAXS and WAXS analysis, and confirmation of the identified co-continuity of the constitutive phases for nominal silica contents greater than 18%wt was obtained by TGA and DMA analysis. While the loss modulus was found to increase monotonically over the entire range of siloxane content, the glass transition temperature exhibited a stepwise increase upon reaching the conditions for phase co-continuity. Molecular dynamics simulations were used to produce model structures for silsequioxanes cage-like structures, as main constituents of the siloxane phase. The predicted interdomain distance between the silsequioxane structures was in agreement with the SAXS experimental data.

Keywords

1. Introduction

Organic-inorganic hybrids obtained via an in situ generation of nanostructures by the sol-gel method are widely studied due to the unique characteristics resulting from their capability to obtain tailored morphologies of the inorganic phase and as potential matrices for composites and coatings applications [Lionetto and Frigione, 2014; Mascia L, 2010; Acebo et al., 2014]. The composition of the precursors, the procedure for the production of epoxy-silica hybrids and the reactions parameters for both organic and inorganic network formation play a fundamental role in controlling the morphology of the inorganic phase and preventing phase separation [Mascia et al., 1998; Mascia et al., 2006; Matejka, 2009; Ochi et al., 2001; Ellis, 1993; Bugnicourt et al., 2007; Ponyrko et al., 2013]. In particular, the formation of the network of one component can exert a control on the reactions and domain growth kinetics of the other component, thereby producing conditions that lead to a wide range of morphologies at the nanometer length scale, including the formation of a co-continuous morphology, as also confirmed by Davis et al. [Davis et al., 2003]. Control of the morphological structure of organic polymer-silica hybrids is generally achieved with the use of functionalized trialkoxysilane coupling agents, as a means of producing covalent bonds in the interphase regions of the organic and inorganic domains [Mascia, 2010].

In a recent study [Afzal et al., 2011] it was shown that bicontinuous epoxy-silica hybrids, obtained with a two-stage procedure, comprising a solvent free hydrolysis step of TEOS and low GOTMS content added to the epoxy resin and cross-linked with a slowly reactive poly(oxypropylene)diamine (Jeffamine D400), will only give rise to a slight increment in the Tg while gross phase separation was experienced at high silica content.

High siloxane content organic-inorganic hybrids based on diglycidyl ether of bisphenol-A (DGEBA) and prehydrolyzed mixtures of tetraethoxysilane (TEOS) and high content of γ-glycidoxypropyl-trimethoxysilane (GOTMS) have recently been produced and extensively characterized by our research group [Piscitelli, et al., 2013]. The large amounts of SiOH groups as well as glycidoxy-silane coupling agents in the siloxane precursor may more effectively improve the interaction with the organic components forming the crosslinked network without any gross phase separation. However, the results have shown that the use of a highly reactive diamine, such as metaxylylenediamine, (MXDA), as hardener for the epoxy resin prevents the full amount of siloxane species in the precursor from participation in the formation of the resulting siloxane network. The resulting epoxy-silica hybrid acquires Tg values lower than that exhibited by the neat epoxy resin cross-linked with the same hardener and with the same molar ratio.

In the present work, the authors examine in more detail the relationship between structure - property of these systems using a low reactivity poly(oxypropylene)diamine hardener, known as Jeffamine D230. In particular, the work was focused on systems with high siloxane contents (up to 40%wt), in which the amounts of silane coupling agent (GOTMS) largely exceeds that of the main silica forming component (TEOS), at weight ratio GOTMS/TEOS = 65/35. In addition to the experimental work, the formation of the nanostructured morphology was simulated by molecular dynamics modeling (MD). Two different atomistic models were used, each constructed to represent the Jeffamine D230 molecule chemically linked to two alkyl silsequioxanes cage-like structures, which were to be formed at high GOTMS contents [Matejka et al., 2000].

2. Experimental section

2.1 Materials

Diglycidyl ether of bisphenol-A (DGEBA) resin with epoxide equivalent weight (EEW) equal to 187 g/moleq was supplied by Shell Chemicals. γ-glycidoxypropyltrimethoxysilane (GOTMS) was supplied by GE Advanced Materials. Tetraethoxysilane (TEOS), dibutyltindilaurate (DBTDL) and the polyetheramine hardener, Jeffamine D230 with an amine equivalent weight of 54.83 g/eq, were purchased by Sigma Aldrich. Distilled water and 2-propanol

were used as solvents for the hydrolysis and condensation reactions of the siloxane precursors. All chemicals were used as received.

2.2 Methods

2.2.1 Synthesis of epoxy-siloxane hybrids

A solution mixture in 2-propanol of GOTMS and TEOS at 1.7:1 molar ratio (65:35 weight ratio) were partially hydrolysed in presence of 0.02wt% dibutyltindilaurate (DBTD) catalyst. The amount of water used for the hydrolysis, expressed in terms of molar ratio with respect to the various components of the mixture, was TEOS : H_2O = 1 : 3, GOTMS : H_2O = 1 : 1.5, 2-Propanol : H_2O = 0.6 : 1.

A 2 wt% HCl/H_2O solution was used to adjust the pH to 6 as a means of increasing the efficiency of the condensation catalyst (DBTDL). The solution mixture was stirred at 60°C for 4 hours and then cooled to room temperature prior to adding the DGEBA monomer. Rotavapor extraction was then carried out at 40°C for 15 minutes in order to remove most of the water and alcohols contained in the mixture. The epoxy hybrid precursor mixture was cooled to room temperature and then the hardener Jeffamine D230 was added in stoichiometric amount with respect to the total epoxy content. The mixture was poured in an aluminium container and cured at 80°C for 4h, followed by a post-cure step at 180°C for 12 hours. These harsh thermal curing conditions were

used to ensure complete reaction of all epoxy groups and the maximum possible level of crosslinks with the siloxane domains. The castings produced were about 1 mm thick. The obtained epoxy-siloxane hybrids were coded Ep-Siy-Je, where y denotes the amount of equivalent silica content (%wt), calculated as the residual amount at 750°C measured trough TGA measurements in air. The obtained values are listed in Table 1, together with the corresponding theoretical siloxane content of the systems examined. The calculated SiO_2 values were the sum of the amount produced from both GOTMS and TEOS, whereas the values of $RSiO_{1.5}$ for the total siloxane content was obtained taking into account the contribution from the organic segment, where R is the glycidoxy propyl chain between silicon atoms and the link to the Jeffamine hardener.

Table 1. Amount of equivalent silica content as residual weight at 750°C and theoretical silica and siloxane content in the different hybrid systems.

Samples	Residual weight in TGA at 750°C[a] (wt%)	Calculated nominal silica content[b] (wt%)	Siloxane content as $RSiO_{1.5}+SiO_2$[c] (wt%)	SiO_2 content from TEOS conversion[d] (wt%)	Siloxane content as $R'SiO_{1.5}+SiO_2$[e] (wt%)
Ep-Je	0	-	-	-	-
Ep-Si7-Je	6.6	10.7	15.2	2.7	19.3
Ep-Si12-Je	12.3	15.7	28.6	5.0	36.3
Ep-Si18-Je	17.8	18.6	41.3	7.2	52.2
Ep-Si22-Je	21.5	22.7	49.8	8.7	63.3

[a] Total silica content after pyrolysis

[b] Theoretical total silica content determined as SiO_2 from TEOS and GOTMS

c) Siloxane content at GOTMS/TEOS molar ratio is equal to 1.7, where R is the glycidoxypropyl segment (MW 115gr/mol)

d) Silica amount obtained from TEOS

e) Siloxane content based on R' as the molecular segment obtained from the reaction of the glycidoxypropyl unit of GOTMS with the Jeffamine D230 (the molar ratio GOTMS/Jeffamine is assumed to be equal to 4)

2.2.2 Characterization Techniques

Fourier transform infrared (FT-IR) spectra were collected in transmission mode over the range 400-4000 cm^{-1} with a resolution equal to 4 cm^{-1} (FTIR, Nicolet). The FT-IR spectra were acquired by depositing a thin film on a KBr disk of the sample examined, both the uncured pristine resin and the hybrid mixture. The reduction of epoxide groups, resulting from the crosslinking reaction with the amine hardener, was monitored in real time both during curing at 80°C for 4h, and in the post-cure step at 180°C for 12 hours.

The conversion degree (α) of epoxide groups was calculated from the equation

$$\alpha = \frac{C_0 - C_t}{C_0} = 1 - \frac{C_t}{C_0} \qquad\qquad \text{Eq. (1)}$$

where C_0 and C_t represent, respectively, the concentration of epoxide groups at the initial and at the generic reaction time t. According to the Lambert-Beer law, the conversion degree α is obtained from the absorbance at 916 cm^{-1} for the epoxide group as:

$$\alpha = \frac{\overline{A}_0^{916} - \overline{A}_t^{916}}{\overline{A}_0^{916}} \qquad \text{where} \qquad \overline{A}^{916} = \frac{A^{916}}{A^{1509}} \qquad \qquad \text{Eq. (2)}$$

The absorbance at 1509 cm^{-1}, assigned to the stretching of aromatic CH groups, was used as the internal reference.

Simultaneous wide- and small-angle X-ray scattering analyses (WAXS and SAXS), for both fully cured and uncured hybrid epoxy samples, were conducted using an Anton Paar SAXSess camera equipped with a 2D imaging plate detector. CuKα X-Rays with 1.5418Å wavelength were generated by a Philips PW3830 sealed tube source (40kV, 50mA) and slit collimated. All scattering data were corrected for background and normalized for the primary beam intensity. In order to remove the inelastic scattering from the data, the SAXS profiles were additionally corrected for both Porod constant and desmearing effect.

Solid-state ^{29}Si-NMR spectroscopy (^{29}Si-CPMAS-NMR) measurements were performed on the cured hybrid samples using a Bruker AV-300 apparatus. NMR spectra were obtained from 12500 scans using the following parameters: rotor spin rate 5000 Hz; recycle time 5 s; contact time 5 ms; acquisition time 33 ms. Samples were packed in 4 mm zirconia rotors with KelF caps. The pulse sequence was applied with a 1H ramp to account for the non-homogeneity of the Hartmann-Hahn condition at high spin rotor rates. Chemical shifts are

related to tetramethylsilane (TMS), using an external sample of tetrakis-trimethylsilyl-silane (TTMSS; up-field signal -135.4 ppm) as secondary reference. The assignment of the NMR bands to the several T_i and Q_i species is as follows: T_0 from -41 to -43ppm; T_1 from -50 to -52ppm; T_2 from -59 to -61ppm; T_3 from -66 to -69 ppm [Matejka et al., 2000], Q_4 at -109 ppm; Q_3 from -101 to -104 ppm,; Q_2 from -93 to -98 ppm; Q_1 from -88 to -90 ppm and Q_0 from -81 to -82 ppm [Brinker et al., 1990]. ^{29}SiNMR analysis provided quantitative data for the fractions of the structural units Qi, corresponding to Si atoms from TEOS with i siloxane bonds (Si–O–Si) and 4-i hydrolyzed groups (Si–OH) as well as for the fractions of the structural Ti corresponding to Si atoms from GOTMS with i siloxane bonds attached to the central atom and 3-i hydrolyzed groups (Si–OH). As reported previously [Piscitelli et al., 2013], the degree of condensation is determined from the distribution of these species. In details the degree of condensation of Q_i species is determined as:

$$[\alpha_{Si}]_Q = \frac{\sum iQ_i}{4} \qquad \text{Eq. (3)}$$

Whereas the degree of condesantion of T_i species is determined as:

$$[\alpha_{Si}]_T = \frac{\sum iT_i}{3} \qquad \text{Eq. (4)}$$

with the fractions of structural units Q_i and T_i obtained by the deconvolution of the ^{29}SiNMR profiles.

Molecular dynamics (MD) simulations were used to obtain theoretical estimates of the distance between neighbouring siloxane domains' as silsequioxanes cage-like structures bonded to Jeffamine D230 through the epoxy groups of GOTMS. Two different atomistic models were constructed to represent the Jeffamine D230 molecule chemically linked to two alkyl silsequioxanes cage-like structures that are expected to be formed at high GOTMS contents [Matejka et al., 2001, Spirkova et al., 2004]. Accordingly, two alkyl silsequioxanes cage-like structures were considered: one bonded via the two terminal $-NH_2$ groups of the Jeffamine molecule (*head-tail junctions*) and another where only one of the two available primary amines are involved in the related reaction (*head-head junction*).

Transmission electron microscopy (TEM) analysis was carried out by using a FEI Tecnai G12 Spirit Twin microscope operated at 120 kV (LaB6 cathode, point resolution 0.35 nm). Images were recorded on a CCD camera with the resolution of 4096×4096 pixels.

A thermogravimetric analysis (TGA) was carried out with a TGA 2950 thermobalance (TA Instruments). Samples were heated from 30 to 750°C at a heating rate of 10°C/min under air flow.

Dynamic-mechanical measurements were performed with a DMA Q800 (TA Instruments) using tensile deformation mode on specimens (7mm wide and 0.5 mm thick) at a grip separation distance of 15 mm. The specimens were heated

11

from -50 to 250°C at a constant heating rate of 3°C/min. The frequency and amplitude of the vibration were set respectively to 1 Hz and ± 5 µm.

3. Results and discussion

In a previous paper [Piscitelli et al., 2013], it was shown that the siloxane component in the "sol" precursor mixture prepared from TEOS and GOTMS at the weight ratio 35:65, immediately after the pre-hydrolysis step at 60°C for 4h, consists of large quantities of T_1, along with varying amounts of T_0, T_2 and T_3 species derived from GOTMS, as well as large quantities of Q_0 species and small amounts of Q_1 species derived from TEOS. These data indicate that the inorganic precursor is only slightly condensed just before mixing with the epoxy resin and, therefore, very rich in Si-OH groups.

In Figure 1a and 1b are shown respectively the FT-IR spectra collected for the pristine epoxy sample during the curing cycle and the conversion degree calculated from the decrease of epoxy peak centred at 916 cm^{-1} with increasing reaction time accordingly to the Eq 1 and Eq. 2 for pristine and hybrid samples. For sake of brevity are not reported FTIR spectra for hybrid samples.
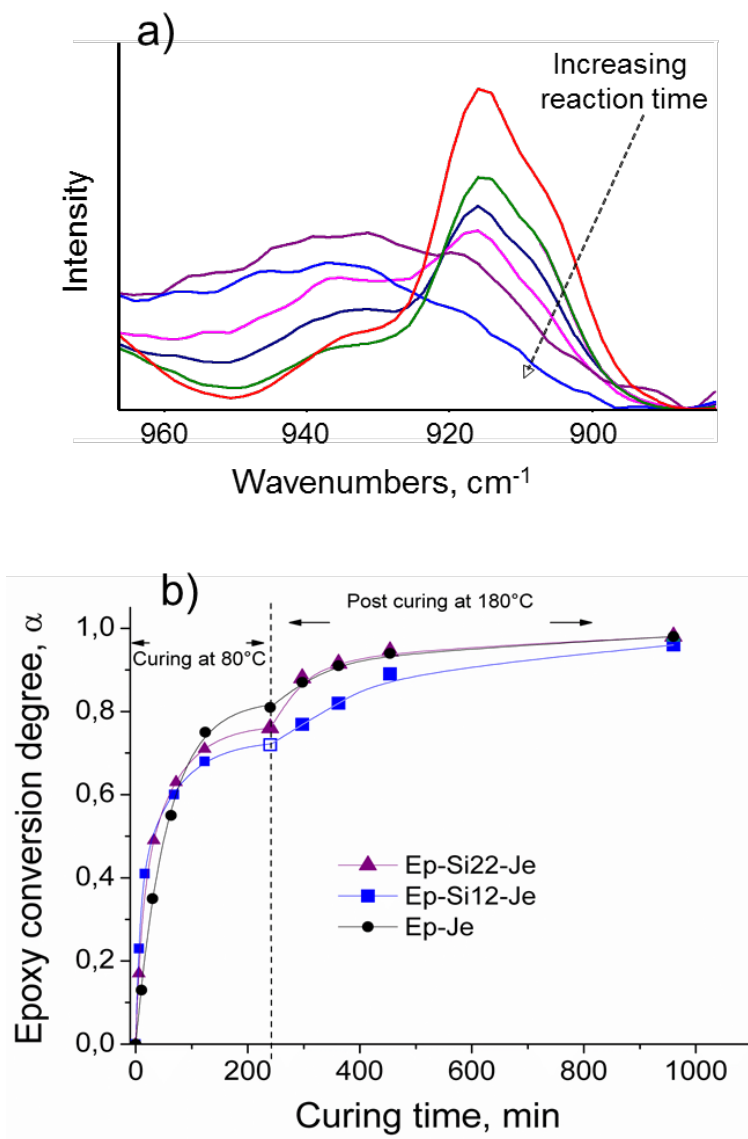
Figure 1. a) FTIR spectra of the pristine epoxy resin during the curing cycle in the region 880-965 cm^{-1}; b) Conversion degree α of the epoxide groups for pristine epoxy resin, Ep-Je, and the hybrid materials EP-Si12-Je and Ep-Si22-Je.

In a previous study [Piscitelli et al., 2013] it was found that, when cross-links are produced with the use of less reactive hardeners, such as Jeffamine, homopolymerization reactions through the opening of epoxy are unlikely to occur evidenced by the total conversion of amine groups in correspondence with the complete consumption of epoxy groups. Therefore, the reduction of the epoxy peak intensity in the hybrid system is ascribed only to reactions between the oxyrane groups in GOTMS with the primary/secondary amines of the Jeffamine hardener. In Figure 1b is shown the comparison of the conversion degree of epoxy groups for the pristine epoxy resin mixture with that obtained for two hybrid systems during both curing (i.e 4h at 80°C) and post-curing (i.e 12h at 180°C). These indicate that at early stage of curing step, the crosslinking reaction rate ($d\alpha/dt$) for the hybrid systems is higher than that of the epoxy resin. This effect is attributed to the presence of free Si-OH groups in the hybrid mixture, acting as catalysts for the reaction between DGEBA and Jeffamine [Mezzenga et al., 2000; Altmann et al., 2001; Ellis, 1993; Bugnicourt et al., 2007] rather than being directly involved in the reaction with epoxy groups present in the reactive mixture [Piscitelli et al., 2013]. The data reported in Figure 1b show that during the first curing step, upon reaching a certain conversion threshold, the cross-link reaction rate in the hybrid systems associated with the reaction of epoxy groups is reduced relatively to the neat epoxy resin. After the post-curing step at 180°C for 12h, however, all samples

14

approach the maximum value for full conversion meaning that all epoxy groups completely reacted with primary and secondary amines of Jeffamine hardener, regardless the siloxane content of the hybrids.

The structural features of siloxane domains obtained by ^{29}Si solid state NMR spectroscopy for selected hybrid systems are shown in Figure 2. These spectra indicate that the inorganic structures present in the different hybrids are not affected by changes in siloxane content, since all systems consist only of T_3, Q_3, and Q_4 units.
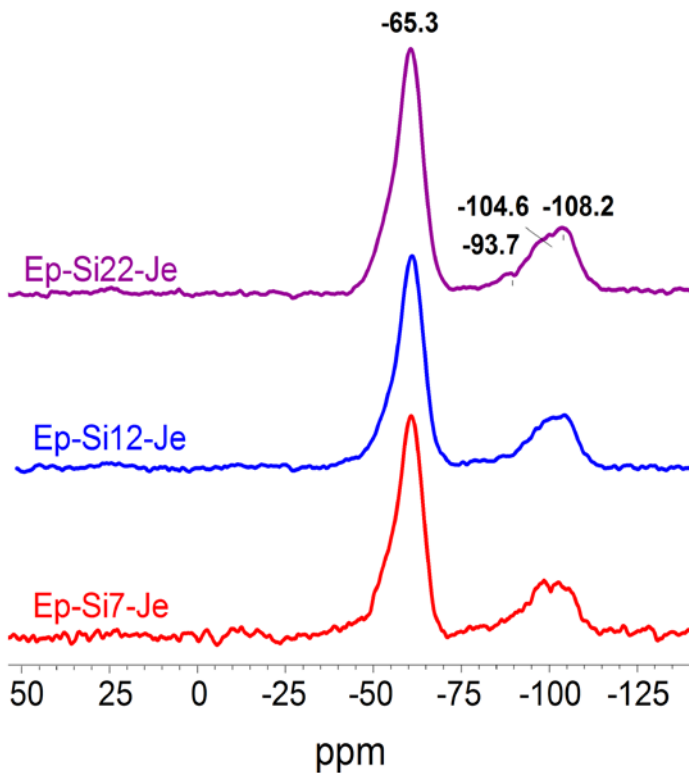
Figure 2. ^{29}Si-NMR spectra of Ep-Si7-Je, Ep-Si12-Je, and Ep-Si22-Je hybrid samples.

The small peak shoulder at about -55 ppm (more pronounced at lower silica content) can be assigned to incomplete condensation of the T_2 units. These spectra confirm that the fractions of Q_3 and Q_4 species and the fraction of T_3 species are about 23% and 67% respectively, and that the conversions of TEOS and GOTMS into siloxane species are independent of hybrid composition. The overall degree of conversion of the siloxane species, estimated as summation of the values for individual components according to Eq. 3 and Eq. 4 reaches values of 90% or higher.

It is important to note that these results are at variance with those reported previously for the same hybrid systems cured with the more reactive metaxylylene diamine (MXDA) [Piscitelli et al, 2013], for which the degree of conversion for the T species was found to decrease with increasing siloxane content, even though TEOS always condense into Q_3 and Q_4 species.

The slower formation of the organic network in the present systems, resulting from the use of a less reactive hardener [Piscitelli et al, 2013], allows the condensation reactions within the siloxane domains to proceed to a higher network density, as confirmed by the large amount of T_3 and Q_3 and Q_4 silicon species present in the system.

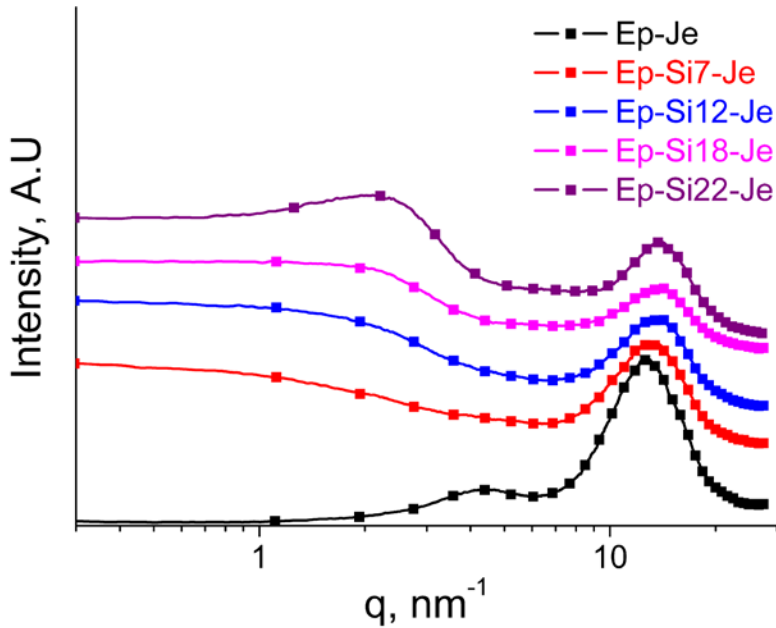The SAXS-WAXS spectra of the hybrid systems over the entire range of siloxane content are shown in Figure 3.

Figure 3. SAXS-WAXS spectra of Ep-Siy-Je hybrid and pristine epoxy samples.

All spectra exhibit a characteristic broad band, centered at scattering vector q values of about 12 nm^{-1} which is attributed, alongside with the peak at about 4 nm^{-1} shown by the pristine resin, to local density fluctuations of the epoxy network [Prado et al., 2005]. These two bands are characteristic of the epoxy resin and do not depend on the hardener employed, as indicated by the very similar results obtained when MXDA was used as hardener [Piscitelli et al., 2013]. Conversely, the spectra of hybrid systems display a change in shape, intensity and position of the broad band at 12 nm^{-1}, as well as the disappearance

of the band at about 4 nm^{-1} which can only be detected as shoulder in the case of hybrids with the lower siloxane content [Dahmouche et al., 1999]. This provides a clear evidence for the substantial structural changes taking place in the structure of epoxy network when the molar amount of GOTMS exceeds that of TEOS in the production of epoxy hybrid systems with high siloxane content. In the SAXS region of the spectra in Figure 3, at q values below 3 nm^{-1}, the scattering intensity changes according to the siloxane content. Specifically, I(q) exhibits the typical Guinier behaviour at low siloxane contents, respectively Ep-Si7-Je and Ep-Si12-Je systems, whereas an overlapped peak is present at 2.33 nm^{-1} for the Ep-Si18-Je and Ep-Si22-Je systems. The presence of a typical Guinier knee is related to the existence of a small siloxane nanostructures dispersed in a dominant epoxy matrix [Zaioncz et al., 2010; Beaucage et al., 1996].

To obtain a better insight into the structure of systems with the low siloxane content, i.e. Ep-Si7-Je and Ep-Si12-Je systems, the slope of the linear region of the $ln(I(q))$ vs q^2 plot was used to determine the gyration radius (R_g) of siloxane domains [Xiong et al., 2004; Yano et al., 1998] according to Guinier's equation

$$I(q) \propto \exp(-q^2 R_g^2 / 3) \hspace{3cm} \text{Eq. 5)}$$

The value of R_g for the siloxane domains of these systems was estimated to be in the region of 0.36 nm, while the geometrical radius is estimated to be equal to 0.46 nm. It is worth recalling that Matejka et al. [Matejka et al., 2000] found

that the condensation reactions of GOTMS lead to formation of cage-like structures corresponding to polyhedral oligomeric silsesquioxane units. The propensity of the system to build up cage-like structures depends on the catalyst used for the sol-gel reactions. In particular, Matejka et al., have shown that due to the tendency of GOTMS to form T_3 structures, cyclic structures are obtained under basic or neutral conditions catalysis, using DBTD as catalyst [Matejka et al., 2001]. Similar conclusions can be drawn for the systems studied in this work on the basis of the ^{29}Si-NMR spectra shown in Figure 2. Accordingly, the T_3 condensed units are the predominant components (i.e about 67% of all siloxane species), whereas the Q_3 and Q_4 units originating from the TEOS are only a limited fraction (i.e about 23% of siloxane species). Furthermore, Sulaiman *et al*. [Sulaiman et al., 2011] have shown that the typical size of octameric silsesquioxanes is about 0.5 nm, which is in excellent agreement with the experimental value of 0.46 nm found for all hybrid systems produced in this work. However, due to the presence of Q_3 and Q_4 species and considering the low amount of silica derived from TEOS with respect to the overall siloxane content (see Table 1), alongside the silsequioxanes structures as $RSiO_{3/2}$ one cannot exclude the formation of both mixed silsequioxanes structures as $RSiO_{3/2}$-$HOSiO_{3/2}$ and dense silica nuclei containing functional T_3 units on the surface. Although it is not possible to establish with certainty the actual structure of the siloxane domains formed during the sol-gel reactions of

TEOS/GOTMS precursor mixture, in the following the siloxane nanostructures can be regarded as siloxanes cage-like nanostructures and, alternatively as glycidoxy surface functionalized siloxane nanoparticles.

In the case of systems with the higher siloxane content, i.e., Ep-Si18-Je and Ep-Si22-Je, a correlation peak appears overlapping the characteristic knee shape of Guinier regime. The position of this scattering peak can be used to estimate the average distance between siloxane nanostructures using the relation $d=2\pi/q_{max}$, where q_{max} is the scattering vector at the peak maximum [Matejka et al., 1998, Xiong et al., 2004; Matejka et al., 2001]. In this case q_{max} is equal to 2.33nm^{-1}, thus the average distance between siloxane nanostructures in these systems is estimated to be around 2.7 nm.

SAXS measurements were also carried out during the course of the thermal curing cycle on the systems with high siloxane content, Ep-Si22-Je, and low siloxane content, Ep-Si12-Je, with the aim to obtain a better understanding of the nature of the interdomain distance peak and the evolution of the inorganic structures. The obtained spectra, shown in Figure 4a, and 4b confirm the tendency of the siloxane precursors to form nanostructures with dimension size in the range 0.4 - 0.5 nm.

The SAXS spectra for the Ep-Si12-Je hybrid (Fig. 4a) show that the characteristic Guinier knee shape, which was already present in samples at the

beginning of the cross-linking reaction, is retained during the entire duration of the cure cycle.
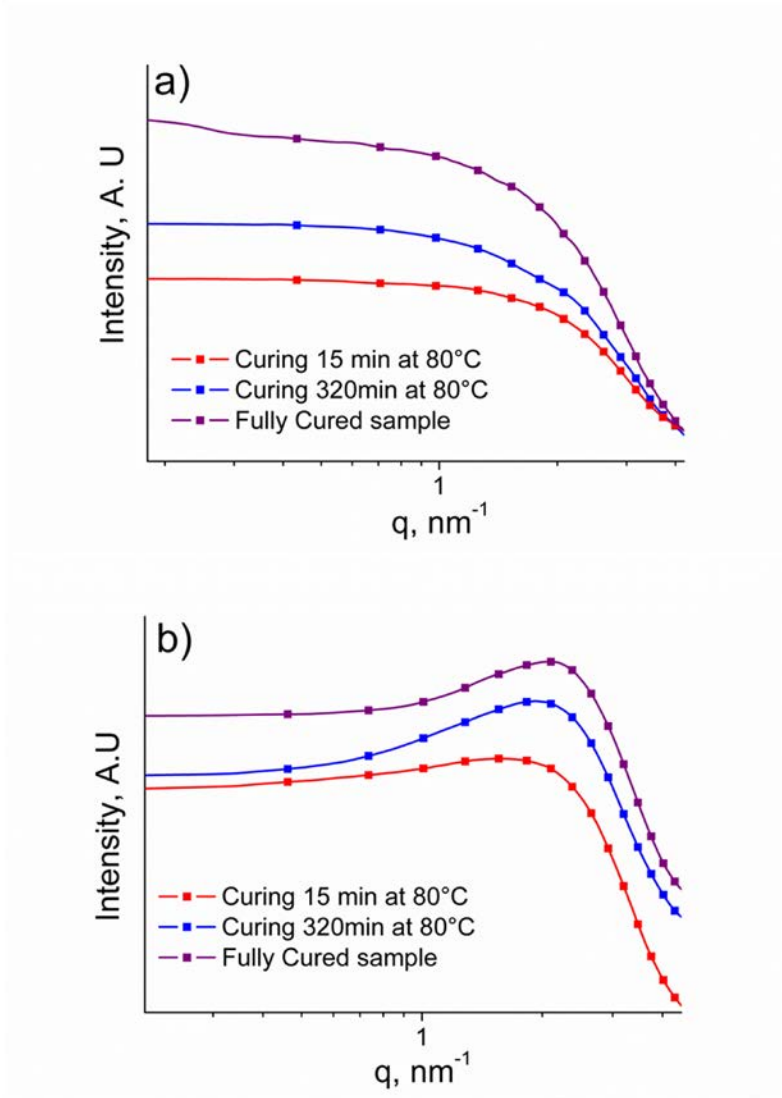

Figure 4. SAXS spectra of a) Ep-Si12-Je and b) Ep-Si22-Je hybrids collected during the curing cycle.

The SAXS data, therefore, indicates that the final morphology of the Ep-Si12-Je sample, consisting of interdispersed nanostructured particulate domains of siloxane species dispersed in the epoxide matrix, is established in the early stages of the epoxy cross-linking reaction. Conversely, for the Ep-Si22-Je sample, a correlation peak appears as a slight shoulder after 15 minutes curing at 80°C and becomes increasingly more evident in the subsequent stages of the cure cycle. The appearance of the correlation peak during the cure cycle is ascribed to the formation of ordered nanostructures [Spirkova et al., 2004]. At higher silica content, i.e., 18 and 22 wt%, the distance between two neighbouring siloxane cage-like nanostructures is sufficiently small to be detected by SAXS measurements. In these systems, the average estimated distance (2.7 nm) is regarded as the distance between heterogeneous siloxane domains separated by the pendant organic substituent γ-(glycidoxy)propyl group bonded to Jeffamine D230. To test the validity of this molecular interpretation, the formation of the nanostructured morphology due to the presence of siloxane cage-like nanostructures was simulated by molecular dynamics modeling (MD). As previously stated, the Jeffamine hardener may bind the epoxy rings of the functionalized nanostructures using either the same $-NH_2$ group twice (*head-head junction*) or the two distinct $-NH_2$ moieties at the two extremes (*head-tail junction*). In the model two Jeffamine molecules were employed, consisting of either 2 or 3 oxypropylene repeating units, which is in

22

the range of the actual system used in which the average number (x = 2.5) of the repeating unit in Jeffamine D230 [Brus et al., 2004]. Moreover, in order to allow for the siloxane cage-like structures to become entrapped in the epoxy network, it has been assumed that each Jeffamine D230 molecule has reacted first the glycidoxy group in the GOTMS and then with a DGEBA unit. This condition has to be satisfied to ensure the uncondensed siloxane nanostructures become anchored in the epoxy network.

These model systems have been used to simulate the events during curing at 80°C, which correspond to the appearance of the correlation peak. From MD calculations it was found that the average distance between two neighboring nanostructures is equal to 3.1 nm, for $x = 3$ and 2.8 nm for $x = 2$ (where x is the number of oxypropylene units present in Jeffamine monomer), when two cages nanostructures are connected by a *head-tail junction.* Therefore, the average value of 2.9 nm was taken as the representative interdomain spacing for head-tail structures. Conversely, when two cages are bound through the same $-NH_2$ group (via a *head-head junction*), the average distance between two neighboring cages is estimated to be equal to 1.8 nm.

In Figure 5 are shown snapshots extracted from the MD calculations for systems where $x = 3$. In particular, Figure 5a shows two cage-like structures bonded through a head-tail junction, while the structure in Figure 5b corresponds to systems with a head-head junction.
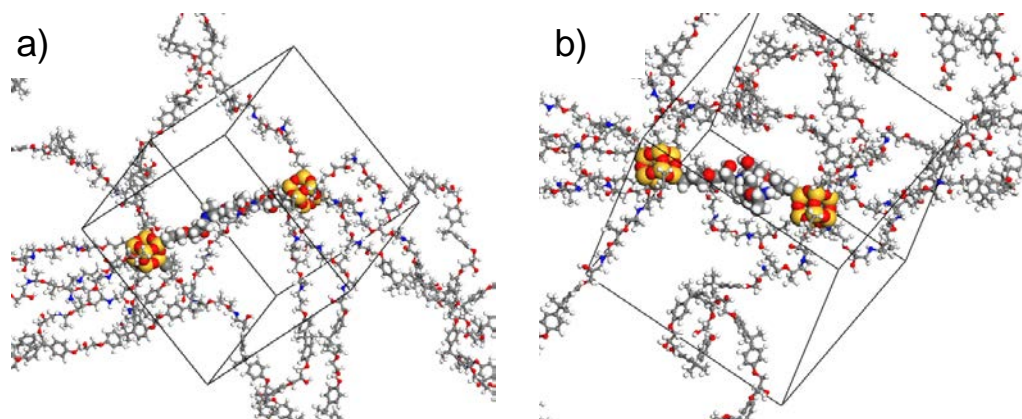
Figure 5. Snapshots extracted from equilibrated molecular dynamics (MD) simulations of the hybrid systems with head-tail (a) and head-head (b) junction. The two silsequioxane cages and the connecting γ-(glycidoxy)propyl-Jeffamine D230 are shown as atom-colored CPK spheres (oxygen, red; silicon, gold; nitrogen, blue; carbon, gray; hydrogen, white) while all other system components are shown as atom-colored sticks-and-balls.

The results obtained from MD calculations indicate that the theoretical estimation of the distance between two neighbouring cage-like nanostructures bonded to the same Jeffamine D230 molecule in the head-tail mode is in good agreement with the experimental value of 2.7 nm obtained by SAXS measurements for the systems with the higher siloxane content. Thus, the distance between two neighbouring cages is determined only by the length of the molecule of the amine hardener that links together the siloxane cages. At the upper end of the siloxane content the number of cage-like structures is

sufficient to allow them to be bonded head-tail to the same Jeffamine D230, giving rise to the formation of a continuous organic-inorganic network.

From the results of the chemical and morphological characterization of the epoxy hybrid materials produced in this study, it can be inferred that the composition of the components and the curing conditions used will induce the formation of highly condensed and rigid cage-like nanostructures bonded *head-tail* via Jeffamine units and exhibiting a high degree of regularity and self-ordering throughout the epoxide network.

Furthermore, the TEM images in Figure 6 reveal the presence of a uniform morphology for both Ep-Si7-Je and Ep-Si22-Je samples.
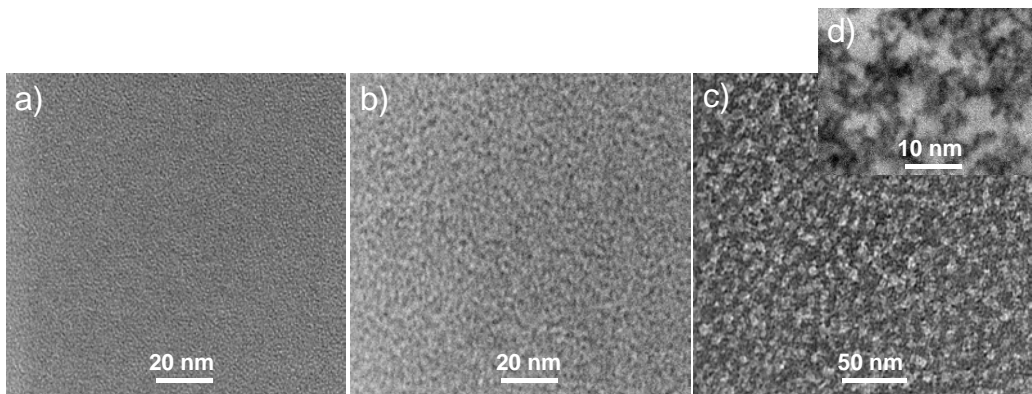

Figure 6. TEM images of a) pristine epoxy, b) Ep-Si7-Je and c) and d) Ep-Si22-Je cured samples.

At low silica contents the hybrid exhibits a finely dispersed morphology, consisting of homogeneous nanostructures embedded in the epoxy matrix. At high silica content, on the other hand, the hybrids are characterized by a coarser morphology consisting of co-continuous siloxane domains. For comparison in Figure 6 is also reported the TEM image of pristine epoxy sample.

In order to confirm the phase co-continuity of the siloxane domains for the Ep-Si22-Je hybrid, thin samples (0.5 mm) were subjected to a stepwise thermal oxidative degradation process. The samples were first placed in an oven for 45 hours at 300°C and then maintained at 400°C for further 45 hours. Since the residue had achieved a constant weight under these conditions it can be presumed that complete ablation of the species has occurred in the epoxide regions residing between the siloxane domains. Figure 7 shows the images of a hybrid sample just after pyrolysis of the organic matter, which clearly reveal that the siloxane residue is much closer to a three-dimensional structure than to powder aggregates (see Figure 7b and c)).
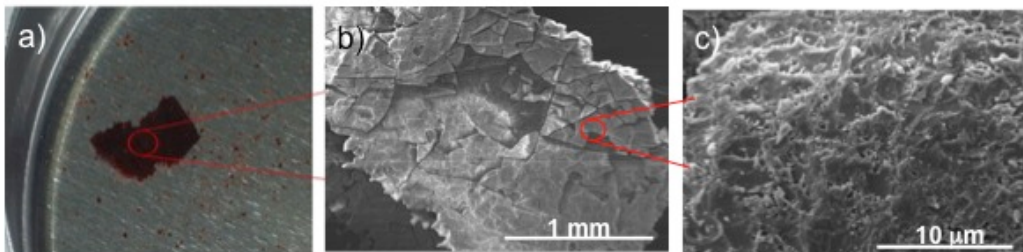

Figure 7. a) Sample in aluminium pan; b) Optical microscope image and c) SEM image of hybrid sample after the pyrolysis cycle.

It should be noted that such a difference in the morphology of the siloxane domains at the two extremes of silica contents is already evident from the data in Table 1. These show that there is a larger discrepancy between the theoretical and experimental silica contents for systems with the lower siloxane contents, which can be attributed the greater loss of silica domains in the gas phase, due to their presence as nanoparticles in the sample.

The thermograms obtained in an oxygen atmosphere (Figure 8) show that at temperature higher than 500°C the thermal oxidative stability of the siloxane-epoxy hybrid materials is in all cases greater than that exhibited by the pristine epoxy resin.
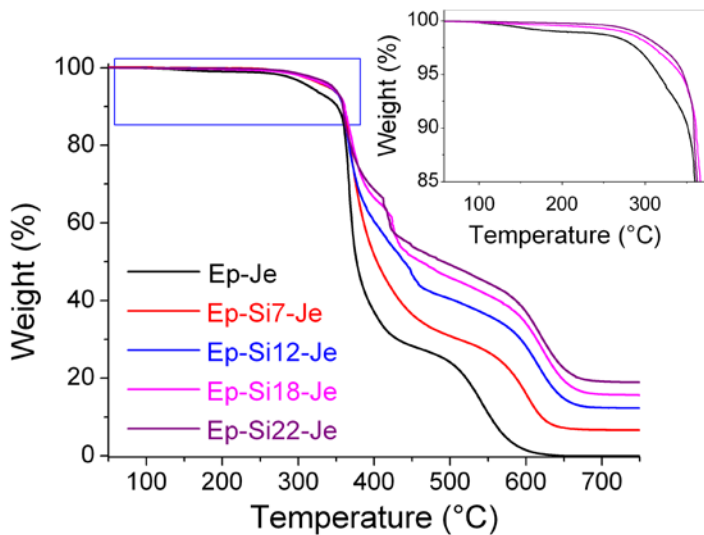

Figure 8. Thermo-gravimetric analyses of pristine epoxy resin and hybrids samples.

However, the samples with the higher siloxane content, EpSi18 and EpSi22, exhibit even a greater stability in the temperature range 380 - 430°C, which is a reflection of the co-continuous morphology of these hybrid systems. An intermediate behavior between dispersed particle and co-continuous phase is displayed by the sample EpSi12-Je, which has an intermediate siloxane content. Valuable information on the morphology and interfaces of organic-inorganic hybrid materials has been obtained by DMA analyses in several reports [Matejka et al., 2000; Mascia et al., 2006]. The epoxy-siloxane hybrids of this study reveal new features in the mechanical spectra, as shown in Figure 9, in terms of variation of storage modulus $E'(T)$ and loss factor $tan\delta$ (inset graph of Figure 9) with increasing temperature.
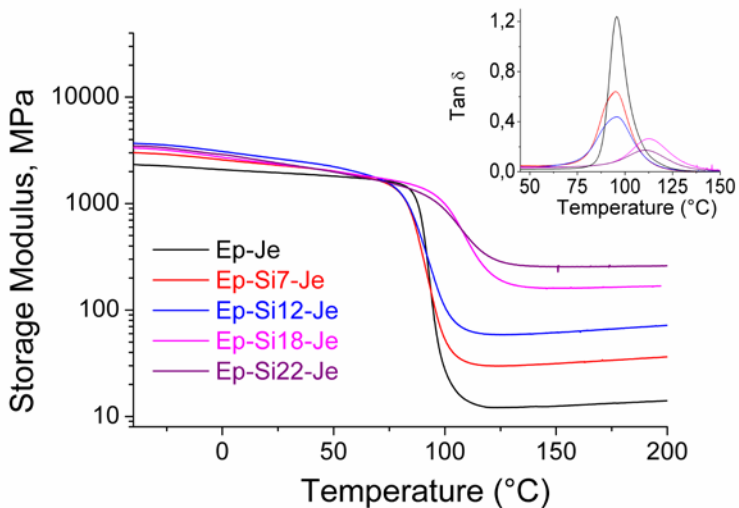

Figure 9. Dynamic mechanical properties of pristine epoxy resin and hybrid samples (in the inset graph the Tanδ as a function of temperature).

In the rubbery plateau region of the spectra the high siloxane systems, Ep-Si18-Je and Ep-Si22-Je, show a very large increase in the modulus relative to the pristine epoxy system (about 20-fold), which can be associated with the highly efficient reinforcement provided by the inorganic network within the co-continuous siloxane domains. Accordingly, the large increase in the storage modulus is accompanied by a large reduction of the loss factor $tan\delta$ (inset graph of Figure 9) and a large increase in T_g (see Table 2). Moreover, it is noted that value of T_g exhibits a sharp rise at equivalent silica contents greater than 12 wt%, which is associated with the threshold conditions for the formation of co-continuous phases.

In Table 2 is reported a summary of relevant data extracted from the mechanical spectra.

Table 2. DMA data for pristine epoxy and hybrid samples

Sample	Tan δ peak temp. (°C)	Storage modulus at 150 $^\circ$ C (MPa)	Tan δ peak values	Loss modulus (E") at Tanδ peak (MPa)
Ep-Je	95.6	12.5	1.2	169.2
Ep-Si7-Je	95.5	31.4	0.64	168.9
Ep-Si12-Je	95.5	61.3	0.44	150.9
Ep-Si18-Je	112.6	160.0	0.26	137.0
Ep-Si22-Je	111.0	255.4	0.17	100.5

In examining the data in Table 2 one observes a clear contrast in the data for samples with siloxane contents respectively below and above the threshold conditions for the onset of phase co-continuity. While the samples with the higher siloxane content show the usual behaviour associated with hybrid systems, the epoxy-siloxane hybrids with low siloxane content, Ep-Si7-Je and Ep-Si12-Je, display a behaviour resembling that expected for particulate filler systems [Mascia et al., 2006]. For these systems the large interparticle distance does not provide an efficient mechanism for the restriction of molecular relaxations within the epoxy network even when the particles are strongly bonded to the matrix. For this reason the T_g remains constant while the filler/matrix interfacial friction gives rise to a slight decrement of the values of the loss modulus, E".

The co-continuity of the siloxane domains at high siloxane contents brings the two phases near to isostrain condition, which correspond to the upper limit for the achievable reinforcing efficiency. While the increase in Tg has frequently been related to the suppression of molecular relaxations within the epoxy network by the siloxane domains, [Lionetto et al., 2013] this may not be the case for the systems of this work in so far as the T_g does not increase further with a larger weight fraction of the siloxane component. This seems in contrast with the changes in both storage and loss modulus, which follow the expected trend from the aforementioned micromechanics argument. Instead it is plausible

that the observed trend in T_g may be related to the densification of the epoxide network brought about by the catalytic effect of the neighboring SiOH groups on the rate of cross-linking reactions and to the high weight fraction of glycidoxy organic siloxane nanostructures (i.e approximately 49.8%wt in the case of the sample Ep-Si22-Je which corresponds to around 64%wt whether also the Jeffamine involved in the head-tail junctions is considered) which modifies the nature of the crosslinked network with respect to the pristine epoxy network (see Table 1). In these systems the T_g is attributed to the relaxation of a well-defined macromolecular segment consisting of siloxane-cage nanostructures connected by Jeffamine in the *head-tail junction* and thus it becomes independent on the epoxy resin content.

Conclusions

In this work it was demonstrated that, through a suitable choice of functionalized siloxane precursor monomers and reaction conditions, it is possible to produce epoxy-silica hybrids whose morphology consists of well-organized cage-like structures interdispersed within the epoxy network. Such cage-like structures form a co-continuous phase upon reaching the threshold siloxane concentration, which is within the range of 12-18%wt nominal silica content for the particular precursor composition of the systems examined. In exceeding the threshold siloxane content, the presence of these structures brings about a large increase in the glass-transition temperature and an enormous reinforcing effect in the rubbery plateau region of the hybrid systems. The experimental results indicate that the use of large quantities of the trialkoxy epoxy silane monomer, GOTMS, is largely responsible for achieving the required conditions through self-organization of the siloxane components during the condensation reactions, forming structures polyhedral oligomeric silsesquioxane structures. Molecular dynamics simulations performed on systems with high siloxane content has made it possible to confirm the mechanism for the formation of the morphological structures identified by SAXS measurements. The *ab-initio* theoretical calculations have revealed that the distance between two neighbouring nanostructures is determined by the chain length of the amine hardener that links them together.

Acknowledgments

References

1. Acebo C, Fernandez-Francos X, Messori M, Ramis X, Serra A, Polymer 2014; 55(20): 5028-5035

2. Afzal A, Siddiqi HM, Polymer 2011:52: 1345-1355

3. Altmann N, Halley P, Cooper J. Mcromol Symp 2001;169:171-177.

4. Beaucage G. J Appl Crystallography 1996; 29:134-146

5. Brinker JC, Scherer GW. In: Academic Press Inc. New York, 1990.

6. Brus J, Spirkova M, Hlavata D, Strachota A. Macromolecules 2004; 37:1346-1357.

7. Bugnicourt E, Galy J, Gerard JF, Barthel H. Polymer 2007;48:1596-1605

8. Dahmouche K, Santilli CV, Pulcinelli SH, Craievich AF. J Phys Chem B 1999;103:4937-4942

9. Davis RS, Brough AR, Atkinson A. J Non-Cryst Sol 2003; 315:197-205.

10. Ellis. Chemistry and technology of epoxy resins, Blackie Academic and Professional, London: Chapman and Hall 1993.

11. Lionetto F, Frigione M. J Appl Polym Sci 2014; DOI: 10.1002/APP.40093

12. Lionetto F, Mascia L, Frigione M, European Polym J 2013;49:1298–1313

13. Mascia L. and Tang T., J. Mat. Chem. 1998, 8:2417-2421

14. Mascia L. In: Functional Fillers for Plastics. M. Xanthos: Wiley-VCH; 2010:Chapter 24.

15. Mascia L, Prezzi L, Haworth B. J Mat Sci 2006; 41:1145-1155

16. Mascia L, Prezzi L, Wilcox GD, Lavorgna M. Progress in Organic Coatings 2006;56:13-22.

17. Matejka L, Dukh O, Brus J, Simonsick WJ, Meissner B. J Non-Crystalline Sol 2000;270:34-47

18. Matejka L, Dukh O, Hlavata D, Meissner B, Brus J. Macromolecules 2001;34:6904-6914.

19. Matejka L, Dukh O, Kolarik J. Polymer 2000;41:1449-1459

20. Matejka L, Plestil J, Dusek K. J. Non-Crystalline Sol 1998;226:114-121

21. Matejka L, in L. Merhari eds., Chapter 1, Hybrid Nanocomposites for Nanotechnology, Springer Science, Business Media, LLC 2009

22. Mezzenga R, Boogh L, Månson JE, Pettersson B. Macromolecules 2000;33:4373-4379.

23. Ochi M, Takahashi R, Terauchi A. Polymer 2001;42:5151-5158.

24. Piscitelli F, Lavorgna M, Buonocore GG, Verdolotti L, Galy J, Mascia L. Macromol Mat Eng 2013;298(8):896-909.

25. Ponyrko S, Kobera L, Brus J, Matejka L, Polymer 2013:54(23):6271-6282

26. Prado LASA, Cascione M, Wichmann MHG, Gojny FH, Fiedler B, Schulte K, Goerigk G. Hasylab Annual Report 2005.

27. Spirkova M, Brus J, Hlavata D, Kamisova H, Matejka L. J Appl Poly Sci 2004;92:937-950.

28. Sulaiman S, Zhang J, Goodson T, Laine RM. J Mater Chem 2011;21:11177-11187.

29. Xiong M, Zhou S, Wu L, Wang B, Yang L. Polymer 2004;45:8127-8139

30. Yano S, Iwata K, Kurita K. Mater Sci Eng C 1998;6:75-90

31. Zaioncz S, Dahmouche K, Soares BG. Macromol Mater Eng 2010;295:243-255.

Table Of Content (TOC)